AIAA JOURNAL
Vol. 48, No. 1, January 2010

Reduced-Order Models for a Shallow Curved Beam Under Combined Loading

S. Michael Spottswood,* Joseph J. Hollkamp,* and Thomas G. Eason*
Air Force Research Laboratory, Wright–Patterson Air Force Base, Ohio 45433

DOI: 10.2514/1.38707

Future U.S. Air Force vehicles require structures that can withstand extreme combined environments. Examples include vehicles exposed to launch, sustained hypersonic velocities, reentry, and stealthy aircraft with buried engines and ducted exhaust. Two of the many conditions that a structure in these environments will experience are elevated temperatures and high acoustic loading. Computational methods are needed to rapidly explore the design space for extreme environment structures. There has been a significant amount of work toward developing reduced-order modeling to address the issue of sonic fatigue. These methods have been demonstrated to be useful for predicting the geometric nonlinear response of aircraft structures to stochastic loading. Recent work also demonstrates that these methods are able to predict the response of planar structures in these combined environments. The present study demonstrates that the implicit condensation reduced-order modeling method can also be extended to curved structures experiencing combined thermal-acoustic loading with changing thermal conditions. Successful displacement and strain comparisons for a curved beam structure are made between results from a commercial finite element code and reduced-order models, using a single random pressure load (162 dB) and varying temperature cases.

Nomenclature

$A_r(i, j, k)$	=	cubic stiffness term in the nonlinear stiffness function
$B_r(i, j)$	=	quadratic stiffness term in the nonlinear stiffness function
$\bar{\boldsymbol{C}}$	=	modal damping matrix
$\boldsymbol{f}(t)$	=	applied force vector
$\boldsymbol{f}_{\boldsymbol{\Delta T}}$	=	thermal force
$\boldsymbol{K}$	=	linear stiffness matrix of the planar structure, including stress stiffening effects
$\boldsymbol{k}_o$	=	linear stiffness matrix of the original structure
$\boldsymbol{K}$, $\bar{\boldsymbol{K}}$	=	general linear stiffness matrices after a thermal-induced geometry change in the physical/modal coordinates
$\boldsymbol{K}_{\boldsymbol{\Delta T}}$	=	linear stress stiffening matrix
$\boldsymbol{K1}$, $\tilde{\boldsymbol{K}}\boldsymbol{1}$	=	quadratic stiffness matrices before and after a thermal-induced geometry change
$\boldsymbol{K2}$, $\tilde{\boldsymbol{K}}\boldsymbol{2}$	=	cubic stiffness matrices before and after a thermal-induced geometry change
$\boldsymbol{M}$	=	mass matrix
n	=	number of modes used in the modal basis
$\boldsymbol{p}$	=	response vector in modal coordinates
t	=	time
$\boldsymbol{w}$	=	vector of relative displacement in physical coordinates
$\boldsymbol{x}$	=	displacement vector in physical coordinates
$\boldsymbol{x_0}$	=	static displacement vector due to a temperature change in physical coordinates
$\boldsymbol{\Delta T}$	=	temperature difference
$\boldsymbol{\theta}$	=	nonlinear internal force vector
$\boldsymbol{\phi}_i$, $\boldsymbol{\Phi}$	=	modal vector, modal matrix
ω	=	linear system natural frequency

Presented as Paper 2235 at the 49th AIAA/ASME/ASCE/AHS/ASC Structures, Structural Dynamics, and Materials Conference and 16th AIAA/ASME/AHS Adaptive Structures Conference, Schaumburg, IL, 7–10 April 2008; received 23 May 2008; accepted for publication 4 July 2009. This material is declared a work of the U.S. Government and is not subject to copyright protection in the United States. Copies of this paper may be made for personal or internal use, on condition that the copier pay the $10.00 per-copy fee to the Copyright Clearance Center, Inc., 222 Rosewood Drive, Danvers, MA 01923; include the code 0001-1452/10 and $10.00 in correspondence with the CCC.

*Senior Aerospace Engineer, Structural Sciences Center.

Introduction

THE goal of the Air Force Research Lab, Structural Sciences Center, is to simulate high-performance aerospace structure in extreme combined environments. Challenges in predicting the response of structures in extreme environments include the coupling between thermal-acoustic-structural response; material nonlinearity; temperature dependence and degradation; spatial variation of material and structural properties; the uncertainty in loads, material properties, geometry, and boundary conditions; and, most relevant to the present study, the computational cost and complexity of large models.

The past decade has seen appreciable growth in the area of dynamic reduced-order models (ROMs) used to predict the response of aircraft structures experiencing sonic-fatigue-type geometric nonlinear response. These models can be derived explicitly [1] and identified from finite element (FE) analysis [2–5] or experimental data [6]. Further, these models have been validated using well-characterized experiments [7,8]. One area of active research is that of curved structures experiencing combined loading. Consider the structural response displayed in Fig. 1. This response represents the normalized transverse displacement at the center of a shallow curved beam experiencing combined transient thermal (20°F/s, 11°C/s) and random pressure loading of 0.3763 $\text{lb}_f/\text{in.}$ (65.93 N/m) from 0–500 Hz. Each half-second time block represents a step increase in temperature of 10°F (5.6°C). The nonlinear dynamic displacement response was generated using ABAQUS [9] implicit Newmark–Beta numerical integration.

In modeling this transient scenario, the beam is assumed to be at the new temperature at the start of each half-second time increment. The beam deforms with the spatially uniform temporally changing thermal conditions, and this deformation is evidenced in the increasing mean center displacement. The structural modes, or eigenvectors, used to populate the basis of a ROM will also change if the response is defined relative to each new reference state. This study initiates an investigation toward using structural modes identified at room temperature, or the cold modes, and extending their use for prediction purposes at these higher temperatures.

Much of the computational and validation studies concerning nonlinear ROMs, as applied to sonic fatigue, have been limited to planar beams and panels. Recent work by Tiso et al. considered curved structures and noted the need for a time-dependent basis in certain circumstances [10,11]. Przekop and Rizzi [12] and Gordon and Hollkamp [13] studied a shallow curved beam with uniformly distributed random loading. An isotropic planar beam is a special

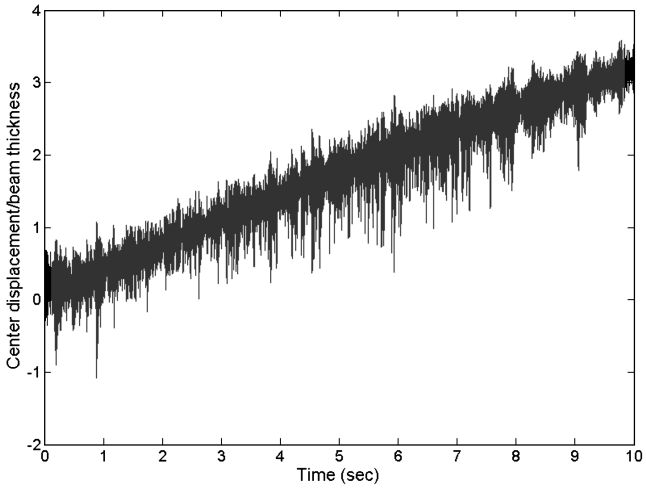

Fig. 1 Displacement response to transient thermal and random pressure loading.

case of the curved beam for which, for negligible in-plane inertial effects, the transverse deflections can be described using bending mode shapes. Przekop and Rizzi [14] have studied the nonlinear response of a flat beam with temperature change using ROMs assembled from cold modes. They demonstrate that for the flat beam, the nonlinear stiffness portion of the ROM does not change with temperature; only the linear stiffness terms change due to stress stiffening. However, curved structures pose an interesting challenge from the perspective of ROM. The axial and transverse degrees of freedom are coupled for both the linear and geometric nonlinear (large deflection) scenarios. The addition of thermally induced stress stiffening results in a change to the physical configuration of a curved structure, as compared with a prebuckled planar structure. Accompanying the change in physical configuration is a change in the structural mode shapes, assuming that this configuration is taken to be the new reference state. The goal of the present study is to investigate the effects of a temperature change on the basis and the resulting ROM of a curved beam. The recently developed IC method is adapted for this task, and an example problem is studied. The results of the problem are discussed to determine the usefulness of a ROM as a predictive tool in this transient thermal scenario.

Reduced-Order Models

The general discretized equations of motion of a structure with geometric nonlinearity, including the effects of temperature, are [14]

$$\boldsymbol{M}\ddot{\boldsymbol{x}} + [\boldsymbol{K}_o - \boldsymbol{K}_{\boldsymbol{\Delta T}} + \boldsymbol{K1}(\boldsymbol{x}) + \boldsymbol{K2}(\boldsymbol{x}, \boldsymbol{x})]\boldsymbol{x} = \boldsymbol{f}(t) + \boldsymbol{f}_{\boldsymbol{\Delta T}} \quad (1)$$

where $\boldsymbol{M}$ is the mass matrix, $\boldsymbol{K}_o$ is the linear stiffness matrix, $\boldsymbol{x}$ is the displacement vector as a function of time, and $\boldsymbol{f}(t)$ is a vector of external time-varying forces. Quadratic and cubic nonlinear stiffness matrices $\boldsymbol{K1}$ and $\boldsymbol{K2}$ are linear and quadratic functions of the nodal displacements, respectively. Stress stiffening due to the temperature change $\boldsymbol{\Delta T}$ is represented by $\boldsymbol{K}_{\boldsymbol{\Delta T}}$. The thermal force is $\boldsymbol{f}_{\boldsymbol{\Delta T}}$.

The response of a flat beam, even with an applied temperature field, can be described using the appropriately scaled unstressed system vibration modes, or the cold modes $\boldsymbol{\Phi}$. Additionally, the nonlinear response of a flat beam can be modeled by using only cubic hardening stiffness coefficients [5], whereas curvature introduces the need for quadratic geometric nonlinearity. The linear stiffness for the system can be represented as

$$\boldsymbol{K} = \boldsymbol{K}_o - (\boldsymbol{\Delta T})\boldsymbol{K}_{\boldsymbol{\Delta T}} \quad (2)$$

In modal coordinates, $\boldsymbol{K}_o$ can be represented as a matrix with the unstressed system frequencies along the main diagonal. The effect of temperature on the response of the flat beam can thus be predicted by recognizing the relationship between $\boldsymbol{K}_o$ and $\boldsymbol{K}$ in modal coordinates for the known values of $\boldsymbol{\Delta T}$. This process will be discussed shortly.

If the static deflection of the structure due to the thermal change is represented by the vector $\boldsymbol{x}_0$, the equations of motion become

$$\boldsymbol{M}\ddot{\boldsymbol{w}} + [\tilde{\boldsymbol{K}} + \tilde{\boldsymbol{K}}\boldsymbol{1}(\boldsymbol{w}) + \tilde{\boldsymbol{K}}\boldsymbol{2}(\boldsymbol{w}, \boldsymbol{w})]\boldsymbol{w} = \boldsymbol{f}(t) \quad (3)$$

where

$$\boldsymbol{w} = \boldsymbol{x} - \boldsymbol{x}_0 \quad (4)$$

The new linear stiffness matrix $\tilde{\boldsymbol{K}}$ contains stress stiffening terms as well as the linear stiffness effects from the change in geometry. The nonlinear stiffness functions $\tilde{\boldsymbol{K}}\boldsymbol{1}$ and $\tilde{\boldsymbol{K}}\boldsymbol{2}$ are also different from the nonlinear functions, in Eq. (1), due to this change in geometry. The linear and nonlinear stiffness may also change due to changes in the elastic properties. The physical displacements are transformed into modal space using the relationship:

$$\boldsymbol{w} = \boldsymbol{\Phi}\boldsymbol{p} \quad (5)$$

where $\boldsymbol{p}$ is a vector of modal amplitudes and

$$\boldsymbol{\Phi} = [\boldsymbol{\phi}_1\boldsymbol{\phi}_2 \cdots \boldsymbol{\phi}_n] \quad (6)$$

is a truncated set of mode shapes. Substituting Eq. (5) into Eq. (3) results in a set of reduced-order equations of motion:

$$\ddot{\boldsymbol{p}} + \bar{\boldsymbol{C}}\dot{\boldsymbol{p}} + \bar{\boldsymbol{K}}\boldsymbol{p} + \boldsymbol{\theta}(p_1, p_2, \ldots, p_n) = \boldsymbol{\Phi}^T\boldsymbol{f} \quad (7)$$

where the modal stiffness is

$$\bar{\boldsymbol{K}} = \boldsymbol{\Phi}^T\tilde{\boldsymbol{K}}\boldsymbol{\Phi} \quad (8)$$

and $\boldsymbol{\theta}$ is a vector function containing the nonlinear terms. A diagonal modal damping matrix $\bar{\boldsymbol{C}}$ has been introduced into the equations of motion at this point. The general form of the nonlinear function for the rth equation is

$$\boldsymbol{\theta}_r = \sum_{i=1}^{n}\sum_{j=1}^{n} B_r(i, j)p_ip_j + \sum_{i=1}^{n}\sum_{j=1}^{n}\sum_{k=j}^{n} A_r(i, j, k)p_ip_jp_k \quad (9)$$

where the $B_r(i, j)$ and $A_r(i, j, k)$ terms express quadratic and cubic modal stiffness, respectively.

The nonlinear function and the modal stiffness matrix depend on the set of mode shapes used in the modal transformation. The mode shapes of the original structure without the thermal load are termed the cold modes. The cold modes will produce a modal stiffness matrix that is nondiagonal for a curved structure at some different temperature. Thus, the modal stiffness matrix cannot be defined solely from the natural frequencies at temperature.

Indirect methods have been proposed in the literature [2–5,12–15] to determine the reduced-order parameters from static solutions of commercial FE packages. By neglecting the dynamic components, Eq. (7) can be rewritten as

$$\sum_{i=1}^{n}\bar{\boldsymbol{K}}(r, i)p_i + \sum_{i=1}^{n}\sum_{j=1}^{n} B_r(i, j)p_ip_j + \sum_{i=1}^{n}\sum_{j=1}^{n}\sum_{k=j}^{n} A_r(i, j, k)p_ip_jp_k = \boldsymbol{\phi}_r^T\boldsymbol{f} \quad (10)$$

for the rth equation. Given a set of static solutions from an FE model, the linear and nonlinear stiffness coefficients can be estimated. Two alternative methods are available. The stiffness evaluation method [4,12,14] uses a set of enforced displacement solutions as the static solutions. Reaction forces are determined from enforced structural displacements that are algebraic sums of the modal shapes. The stiffness coefficients can be determined from the reaction forces by an algebraic procedure. The method must include membrane dominated modes in the basis to accurately capture the effects of structural stretching. A second method, the IC method [2,3,5], uses applied loading for the static solutions. Loads derived from scaled combinations of the mode shapes are applied to the FE model and the

resulting displacements are determined. The effects of membrane stretching are implicitly contained in the displacements. Membrane modes need not be included in the modal basis. The coefficients are then estimated from the solution in a least-squares procedure.

The IC method is easily adapted to estimate the linear coefficients as well as the nonlinear coefficients of Eq. (10). However, multiple levels of the applied load are now necessary to accurately estimate the parameters. In addition, the cubic terms involving three modes in Eq. (10) were ignored to reduce the number of parameters in the estimation process. Those terms are in some sense redundant, because the model still has the ability to couple three modes without them.

In the past, an expansion procedure has been added to the IC method to recover membrane displacements for flat structures [15]. The expansion procedure was also applied to improve the results for curved structures [13]. The expansion procedure was based on the observation that a model containing bending and membrane modes could be condensed to a model containing only bending modes. The modal condensation procedure suggested an analogous expansion procedure. When cold modes are used with curved structures at temperatures as described in Eq. (7), models containing both bending and membrane modes will have linear modal stiffness coefficients that denote significant linear bending-to-membrane coupling. These terms are assumed to be negligible in the condensation procedure, and hence the expansion procedure is suspect and is not used in this paper. Fortunately, the case for an expansion procedure required to recover membrane displacements for a curved structure is not as strong as that for a planar one. A curved structure modeled in the Cartesian coordinate system will have bending mode shapes that contain both in-plane and out-of-plane displacements. The bending mode shapes do not contain pure bending terms but are rather bending dominated mode shapes. Some of the stretching is spanned by the bending mode shapes (basis). Thus, the expansion procedure is not necessary to describe all the membrane displacements. The work in [16] describes how the expansion procedure can be applied to this problem.

Example Problems

First, consider the case of the flat beam, including the effects of temperature [12]. The beam geometry is shown in Fig. 2. The beam length, width, and thickness are 18.0, 1.0, and 0.09 in. (0.46, 2.54×10^{-2}, and 2.28×10^{-3} m), respectively. The beam is aluminum, with elastic modulus of 10.6×10^6 psi (73.1 GPa), shear

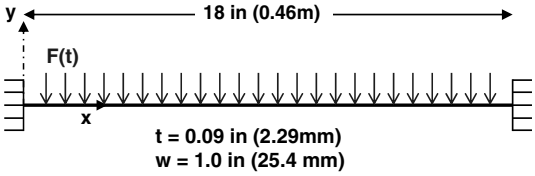

Fig. 2 Flat beam geometry.

modulus of 4.0×10^6 psi (27.6 GPa), density of 2.588×10^{-4} $\text{lb}_f \cdot \text{s}^2/\text{in.}^4$ (2768 kg/m^3), and a thermal expansion coefficient of 12.4 $\mu \cdot \text{in./in./°F}$ (23 $\mu \cdot \text{m/m/°C}$). The material properties were assumed to remain constant for all cases.

The cold modes used in the basis, the first four bending modes, have frequencies of 57.8, 159, 312, and 516 Hz, respectively. The modes were obtained from an ABAQUS beam model. The modal equivalent of $\boldsymbol{K}$, in Eq. (2), or $\bar{\boldsymbol{K}}$ for a $\boldsymbol{\Delta T}$ of 35°F (19°C) was evaluated in the present study using linear FE results with an applied uniform temperature field constant through the thickness. Then, $\bar{\boldsymbol{K}}$ for $\boldsymbol{\Delta T} = 70°\text{F}$ (39°C) was evaluated.

For a prescribed change in temperature $\boldsymbol{\Delta T}$, the total linear stiffness matrix $\bar{\boldsymbol{K}}$ can be assembled from the system frequencies. Because $\bar{\boldsymbol{K}}_o$, the unstressed linear modal stiffness matrix is $\bar{\boldsymbol{K}}$ for $\boldsymbol{\Delta T} = 0°\text{F}$, the matrix $\bar{\boldsymbol{K}}_{\boldsymbol{\Delta T}}$ can now be calculated. The modal stiffness $\bar{\boldsymbol{K}}$ at different temperatures is determined and used for postbuckling predictions of the flat beam. Equation (2) in modal coordinates is the multimode equivalent to the single-mode representation, detailed in Lee [17] and Yang et al. [18]. Predictions at different random loadings are now possible, given the temperature-dependent linear stiffness matrix and the identified cubic nonlinear stiffness coefficients [the A_r terms in Eq. (10)]. Figure 3 displays the center displacement results of a four-mode model of the flat beam with a constant $\Delta T = 70°\text{F}$ (39°C). Broadband uniformly distributed random (in time) loading was applied to the beam between 140 and 170 dB (reference pressure2.9×10^{-9} psi, 20 μPa). Notice that the persistent snap-through response does not occur until 164 dB. Before 164 dB, the response remains at a single equilibrium state. Figure 4 displays the power spectral density (PSD) of the prediction from the four-mode model at $\Delta T = 70°\text{F}$ (39°C) subjected to 164 dB, as compared with ABAQUS implicit nonlinear dynamic results. The flat beam FE model consisted of 144 B31 beam elements. The results show that the four-mode model is an accurate approximation for excitations with frequencies up to

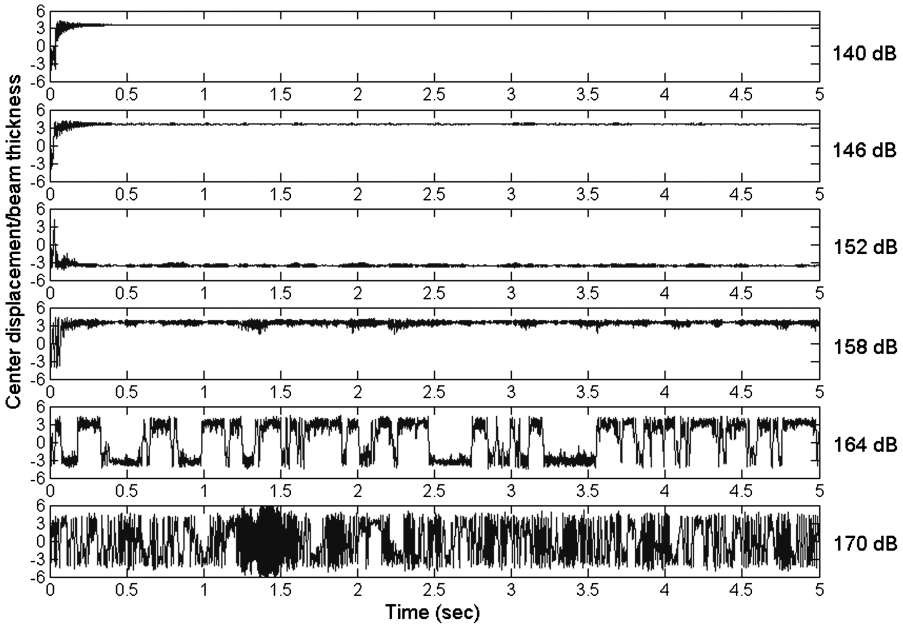

Fig. 3 The center displacement of the flat beam for $\Delta T = 70°\text{F}$ (39°C).

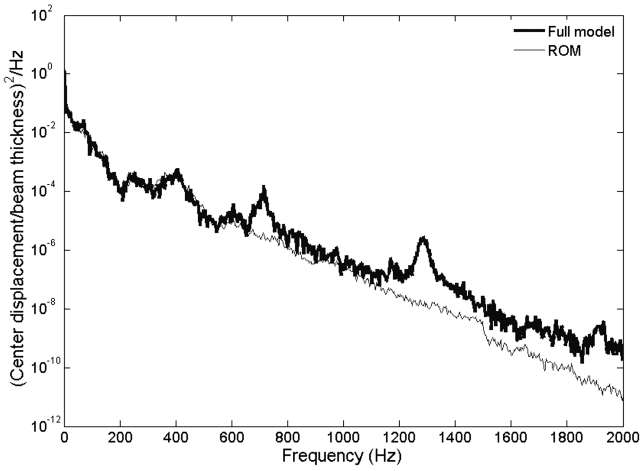

Fig. 4 The PSD of the center displacement of the beam at $\Delta T = 70°$F (39°C) and 164 dB.

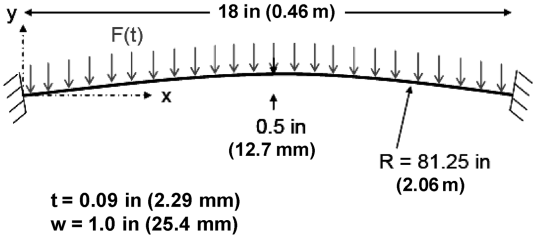

Fig. 5 Curved beam geometry.

500 Hz, even though the beam experiences snap-through dynamic instabilities.

The use of the IC method for curved structures experiencing different thermal conditions will be investigated via the following clamped–clamped curved beam example, displayed in Fig. 5. This configuration is well documented in the literature [12,13]. The beam projected length, width, and thickness are 18.0, 1.0, and 0.09 in. (0.46, 2.54×10^{-2}, and 2.28×10^{-3} m), respectively. The radius of curvature is 81.25 in. (2.06 m). The beam material properties are the same as for the flat beam case and, again, the material properties for the curved beam were assumed to remain constant for all the thermal cases.

In the present study, five different thermal cases were considered. The mode shapes for these cases are displayed in Fig. 6. One random pressure load case with a root mean square (RMS) equal to 0.3763 lb_f/in., 65.93 N/m (162 dB), with a flat spectrum between 0–500 Hz, was used. Mass proportional damping provided 2.0% damping at 258 Hz, the frequency of the first symmetric cold mode. An ABAQUS FE model with 144 B31 beam elements was used to compare with the ROMs. The numerical data used in the comparison were generated using ABAQUS direct nonlinear implicit integration, with a time step of 5×10^{-5} s. Each ABAQUS run required approximately 12.7 h on a 2 GHz dual-core processor computer with 8 GB of RAM. Only a single CPU was used for each ABAQUS job.

Consider Fig. 6, the first four bending mode shapes of the beam as a function of temperature. Notice that there is very little change from the unstressed state to $\Delta T = 50°$F (28°C). However, when ΔT is greater than 50°F (28°C), there are appreciable differences in the modes. Further note that the order of the modes changes at $\Delta T = 150°$F (83°C). At this temperature difference, the curved beam has closely spaced roots.

The comparison of mode shapes suggests that there may be temperature regimes for which a constant basis may not be sufficient for broad temperature regimes. For instance, note that a basis assembled from the cold modes provides only a single mode with significant deflection at the beam center: mode 2. Mode 3 does offer a small amount of deflection at the beam center. Can this basis describe motion at elevated temperatures, for which the center deflection is described with a greater number of modes? In Fig. 7, PSDs of the center displacement of the curved beam, generated using ABAQUS, are shown. Notice the difference in displacement frequency content as the temperature increases. In the frequency band of 0–500 Hz, only the response at $\Delta T = 0°$F is dominated by a single peak. Interestingly, notice that the RMS displacement for a $\Delta T = 100°$F (56°C) and 150°F (83°C), adjusted for the increased mean displacement, is nearly the value at $\Delta T = 0°$F. This displacement then decreases for a $\Delta T = 200°$F (111°C).

ROMs for the five thermal cases were created using the four cold modes ($\Delta T = 0°$F), shown in Fig. 6. The results from 132 static load cases were obtained from ABAQUS. The models were created using the IC method, programmed using MATLAB [19]. Each ROM was subjected to the distributed random loading used with the full model simulation. Twenty s time records were computed using a Newmark time integration procedure, programmed in MATLAB with a time step of 2×10^{-5} s. Each time record required 80 s of CPU time on a computer configured identically as that used on the ABAQUS simulation. The computation time required to complete the 132 static load cases was trivial in the present example, but it is expensive for

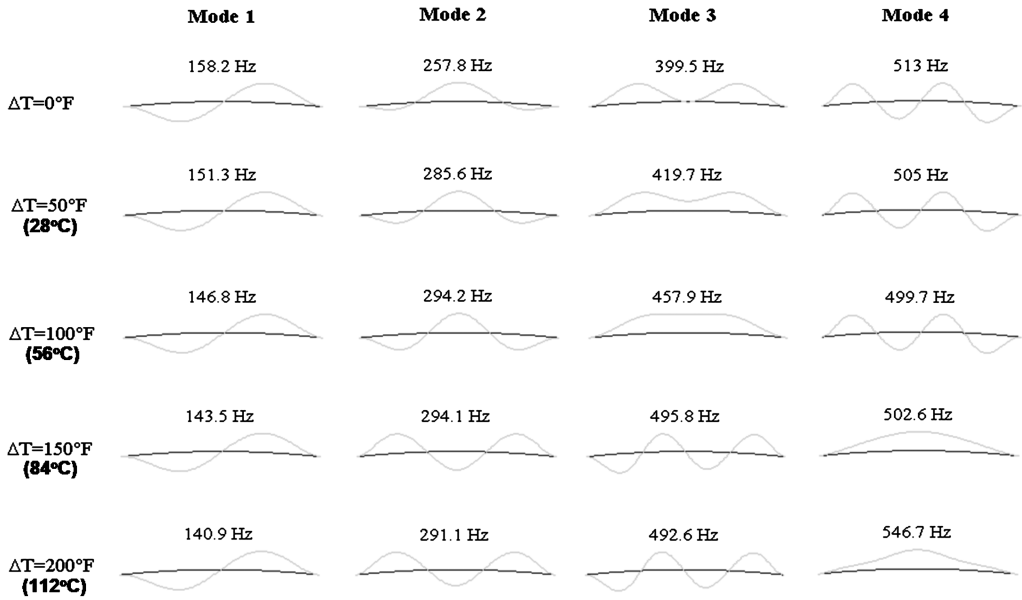

Fig. 6 The first four mode shapes for the curved beam, as a function of temperature.

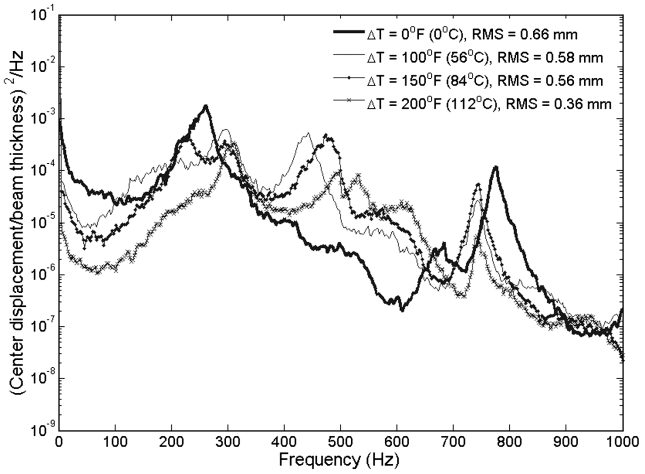

Fig. 7 Curved beam center displacement from ABAQUS.

realistic aircraft panels. The resulting modal displacements were then transformed to physical coordinates using the modal vectors. The ROMs were used to predict the transverse displacement at the beam center and the displacement of the x direction and the y direction at the quarter point of the beam. Additionally, predictions were made of the total strain at the top surface of the beam at a point slightly less than the quarter point, or 3.68 in (0.093 m). These results were compared with the ABAQUS results for $\Delta T = 0$, 100, 150, and 200°F (0, 56, 83, and 111°C).

The predictions for the transverse displacement at the beam center are shown in Fig. 8. Predictions from the ROM are labeled as such, and the ABAQUS time integration results are labeled as full model. As expected, the ROM can predict the displacement at $\Delta T = 0$°F because the basis was constructed with mode shapes from that temperature. The response contains a single peak in the 0–500 Hz band. Of the four cold modes used, note that only the second mode shape has a nonzero transverse displacement at the beam center. Yet, as the temperature changes, the ROM can accurately predict the multimodal nonlinear behavior of the beam center displacement.

The predictions for the x and y displacements at the beam quarter point are shown in Fig. 9. Again, as we would expect, the ROM can predict the displacement at $\Delta T = 0$°F because the model was assembled using modes from that temperature. The predictions at the other temperature conditions are good as well, but the comparisons degenerate as the temperature difference increases. The y-direction predictions appear better than the x-direction predictions. The x-direction displacements require a better membrane basis set, which is not available using the IC method (given the present circumstances).

The strain predictions (at $x = 3.68$ in., 0.093 m) along the beam x axis are shown in Fig. 10. Again, the ROM predicts the strain accurately at $\Delta T = 0$°F. The predictions at other temperature conditions are generally good but also deteriorate with increasing temperature change. The strain predictions are not nearly as accurate as the displacements, as strain is derived from the displacement predictions. The strain prediction would improve with a more representative basis set.

Presumably, a larger basis would be an improvement. To this end, an eight-mode ROM was built using the first eight cold modes. The predictions for $\Delta T = 150$°F (83°C) are shown in Fig. 11. The predictions improve outside the 0–500 Hz band but not appreciably inside the band. In particular, the prediction of the x-direction displacement at the quarter point did not improve. The additional four modes are predominantly bending modes and did not improve the ability to predict membrane displacements.

Figure 12 shows the predictions for a four-mode ROM built with warm modes (i.e., the modes at the temperature/reference state of interest). The predictions improve over the cold mode predictions as expected. The warm basis was assembled with modes from the new reference state. Most notably, the x-direction displacement at the beam center improved, indicating that use of the warm modes improves the ability to predict membrane displacements without the use of normal membrane modes in the basis.

It was noted earlier that the stiffness terms in Eq. (3) change with temperature. Specifically, the linear stiffness terms accounts for

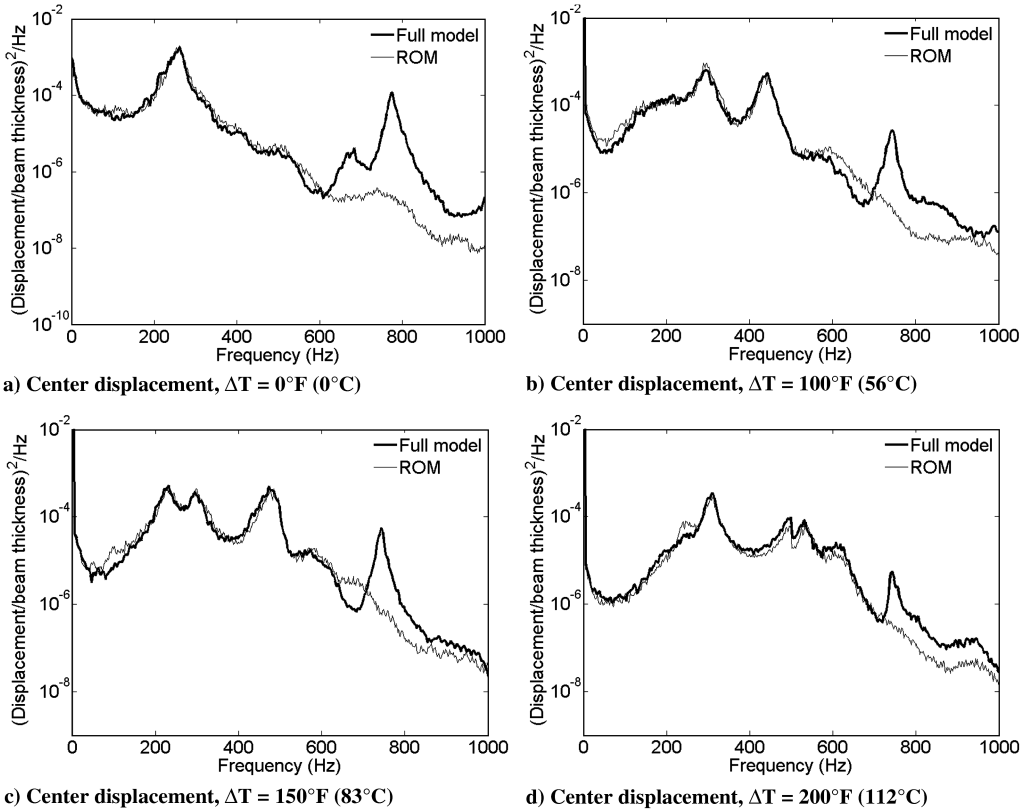

a) Center displacement, ΔT = 0°F (0°C) **b) Center displacement, ΔT = 100°F (56°C)**

c) Center displacement, ΔT = 150°F (83°C) **d) Center displacement, ΔT = 200°F (112°C)**

Fig. 8 Prediction of transverse displacement at the beam center for various temperatures using four cold modes.

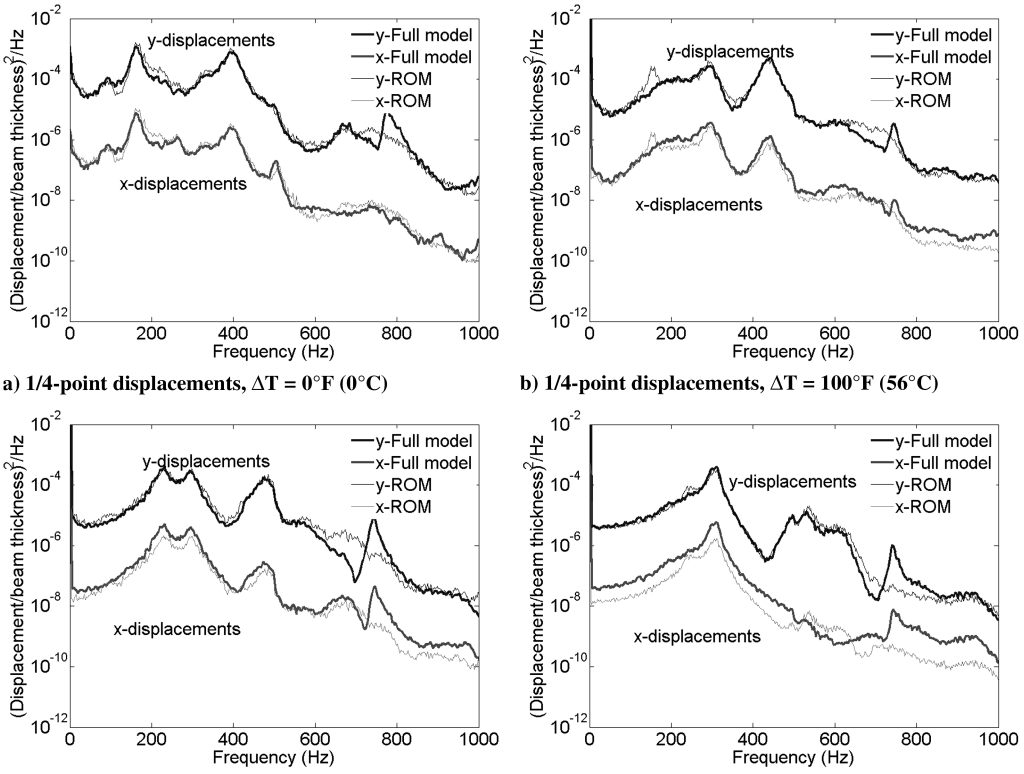

a) 1/4-point displacements, ΔT = 0°F (0°C)

b) 1/4-point displacements, ΔT = 100°F (56°C)

c) 1/4-point displacements, ΔT = 150°F (83°C)

d) 1/4-point displacements, ΔT = 200°F (112°C)

Fig. 9 Prediction of curved beam quarter-point displacement at various temperatures using four cold modes.

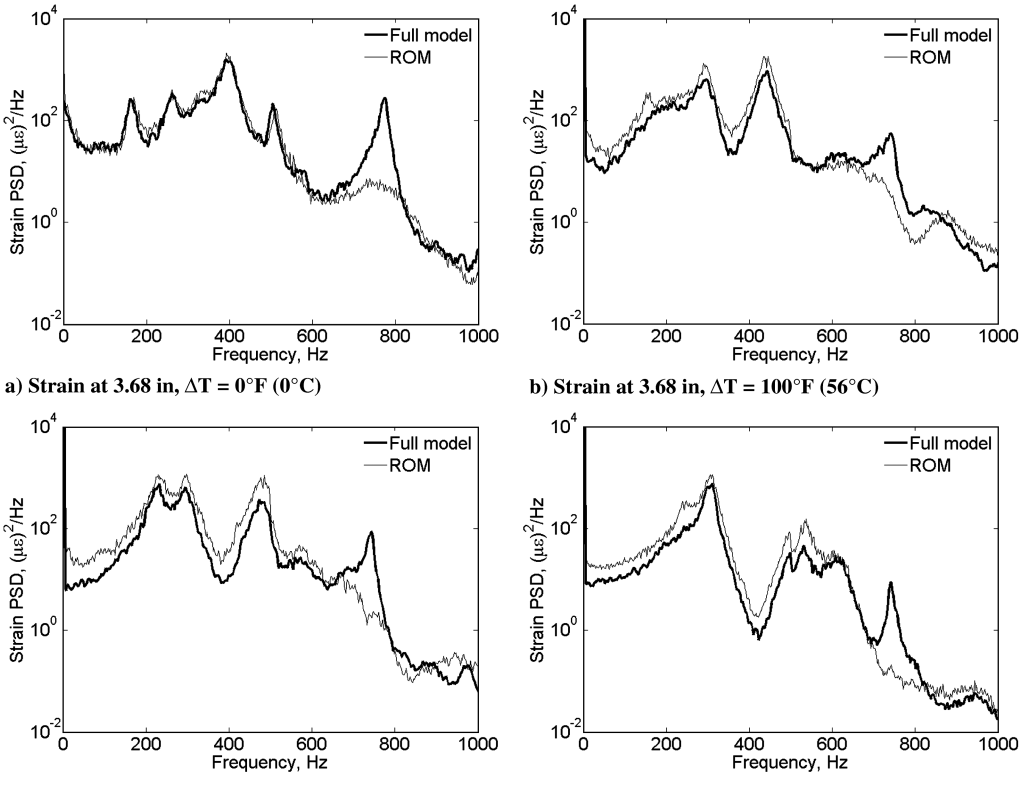

a) Strain at 3.68 in, ΔT = 0°F (0°C)

b) Strain at 3.68 in, ΔT = 100°F (56°C)

c) Strain at 3.68 in, ΔT = 150°F (83°C)

d) Strain at 3.68 in, ΔT = 200°F (112°C)

Fig. 10 Prediction of curved beam strain at various temperatures using the cold modes.

stress stiffening, whereas the nonlinear stiffness terms change as a function of the change in geometry. One issue to consider is the effect of temperature on the identified linear and nonlinear coefficients. In Fig. 13, linear stiffness terms (ω^2 on the main diagonal for zero ΔT), identified when using the cold mode basis, are displayed as a function of temperature. Note that the offdiagonal term $K(2, 3)$ is nonzero once a ΔT is introduced. This indicates that the cold mode basis no longer results in a diagonal linear stiffness matrix. This was expected, because the cold mode basis was used to identify the coefficients.

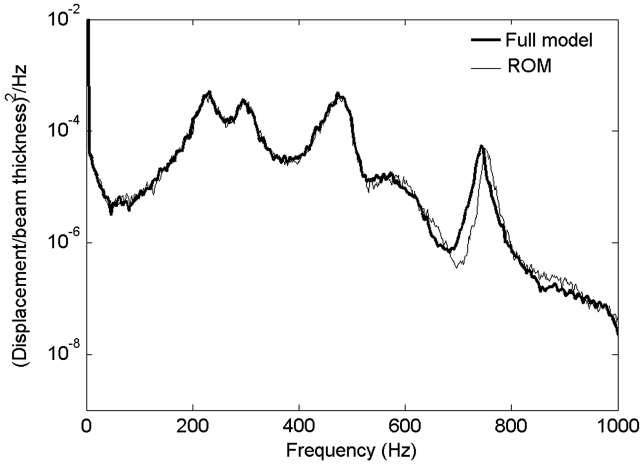

a) Center displacement, ΔT =150°F (83°C)

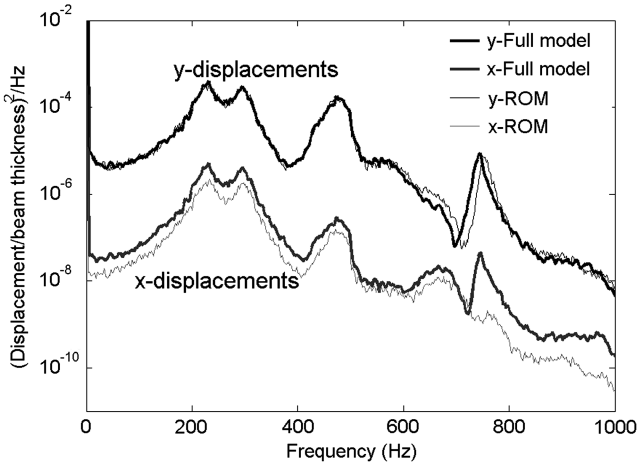

b) 1/4-point displacements, ΔT = 150°F (83°C)

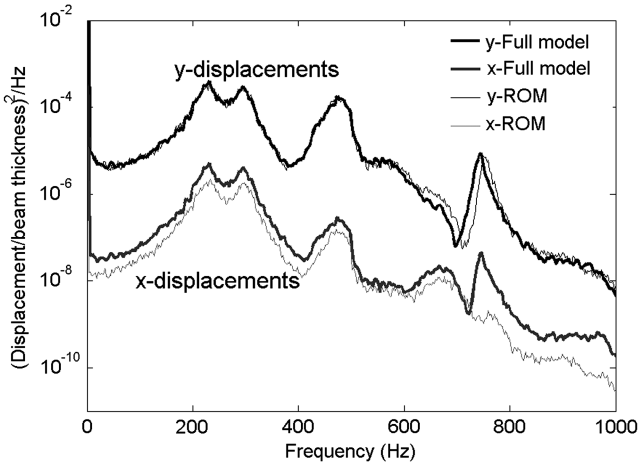

c) Strain at 3.68 in, ΔT = 150°F (83°C)

Fig. 11 Predictions using an eight-mode ROM, built with cold modes, compared with full-order model results.

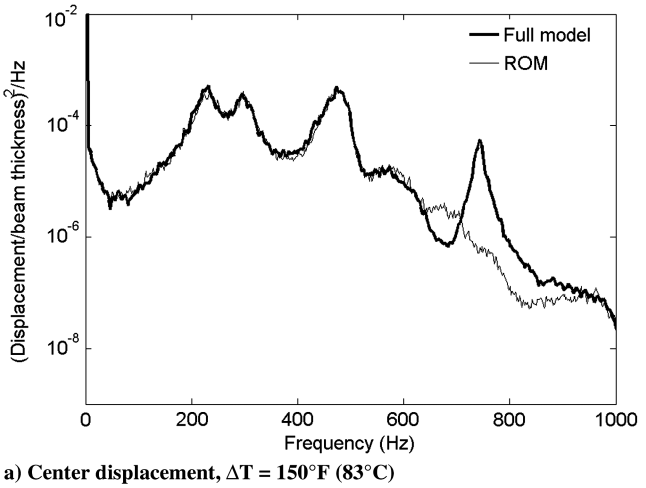

a) Center displacement, ΔT = 150°F (83°C)

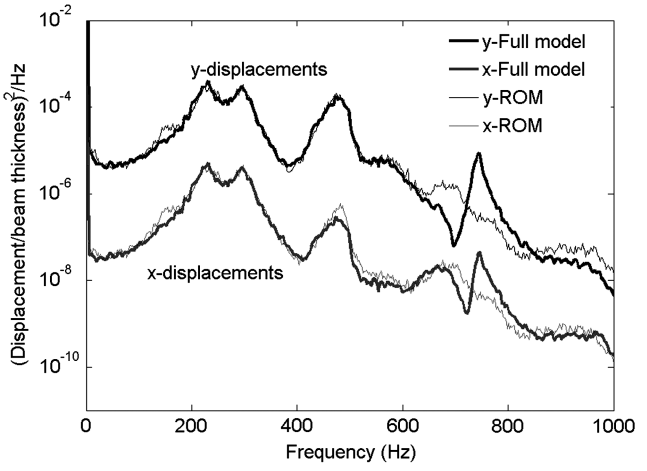

b) 1/4-point displacements, ΔT = 150°F (83°C)

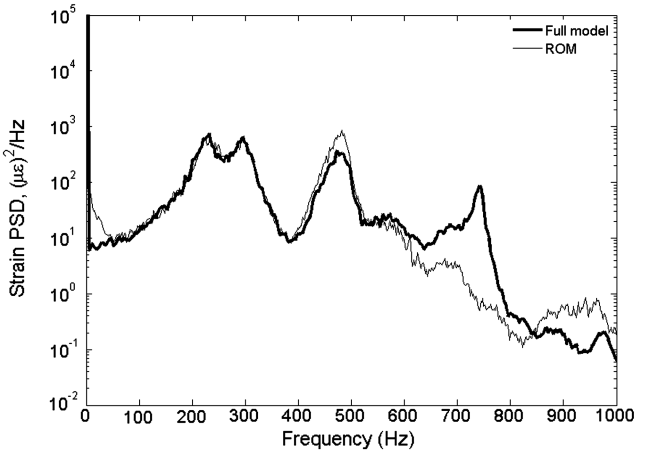

c) Strain at 3.68 in, ΔT = 150°F (83°C)

Fig. 12 Predictions using a four-mode ROM, built at temperature, compared with full-order model results.

Figures 14 and 15 display a sampling of the quadratic and cubic coefficients, identified using cold modes, for the second mode equation [i.e., $r = 2$ in Eq. (10)]. In both cases, the terms have been normalized with the respective cold ($\Delta T = 0$°F) coefficient. Additionally, the samplings of quadratic terms displayed were all greater than 1×10^8, whereas the cubic terms displayed were all greater than 1×10^{10}. Note that the quadratic terms appear to vary linearly with the temperature. Recall that the quadratic coefficients depend upon the curvature. The same cannot be said of the cubic terms. This is the disadvantage in using a varying basis (i.e., reference state). This issue is addressed in [16].

Conclusions

Computational methods are needed to rapidly explore the design space for structures in extreme environments. ROM methods have been demonstrated to be useful for predicting the geometric nonlinear response of aircraft structures to random fluctuating pressure loadings. Recent work has also shown that these methods are sufficient for predicting the response of planar structures in combined thermal-acoustic environments. The present study demonstrates that a ROM can also be extended to curved structures experiencing combined thermal-acoustic loading. One difficulty associated with curved structures is the change in geometric

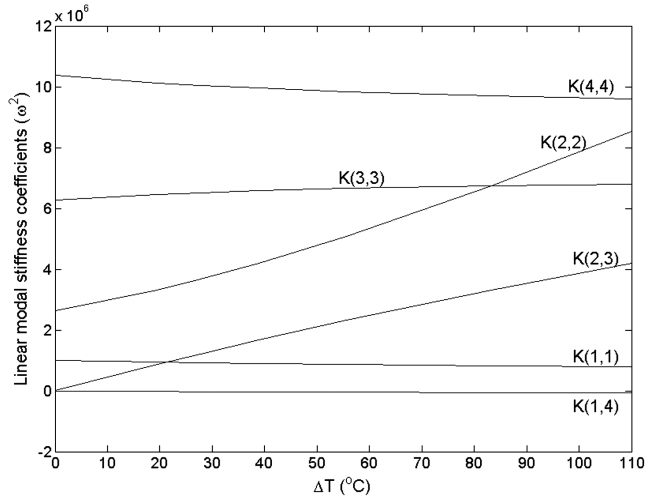

Fig. 13 Representative linear stiffness terms as a function of temperature.

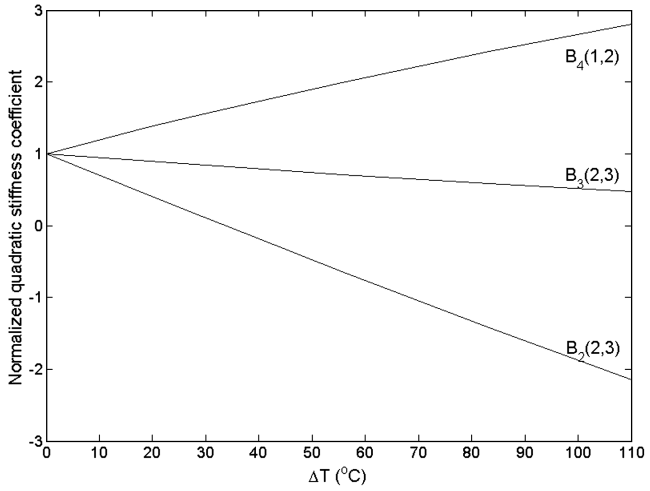

Fig. 14 Representative normalized quadratic stiffness terms as a function of temperature.

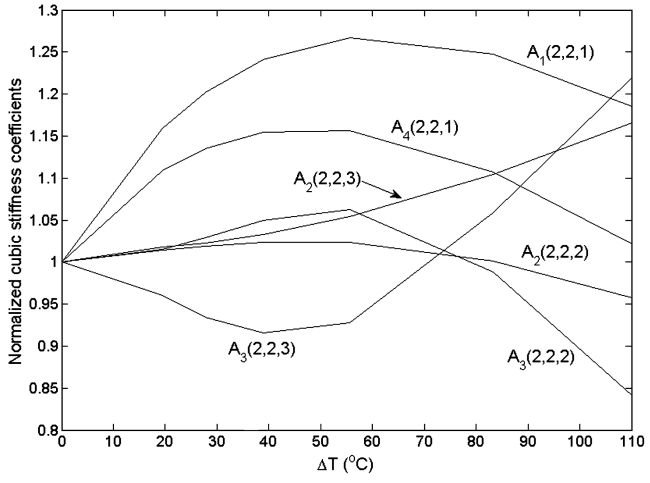

Fig. 15 Representative normalized cubic stiffness terms as a function of temperature.

configuration with accompanying thermal changes. If the structural reference state is assumed to change, then the normal modes will also change with the temperature. The results of this study show that some accuracy would be lost with this scheme, but the predictions are of sufficient fidelity for exploration of the design space.

The IC method was used in this study, and only bending modes were used in the basis. In the past, an expansion procedure allowed the IC method to recover membrane displacements. However, when cold modes are used with curved structures at temperature, the expansion procedure will not work. Fortunately, a curved structure, when modeled in the Cartesian coordinate system, will have bending mode shapes that contain both in-plane and out-of-plane components. Some of the structural stretching is spanned by the bending mode shapes. Thus, the expansion procedure is not fully necessary to obtain membrane displacements. Extending the modal basis should also improve the predictions. However, the results in this study did not show remarkable improvement when the modal basis was increased from four to eight cold modes. The best predictions were obtained when warm modes, the mode shapes at temperature, were used in the construction of the ROMs.

References

[1] Shi, Y., and Mei, C., "A Finite Element Time Domain Modal Formulation for Large Amplitude Free Vibrations of Beams and Plates," *Journal of Sound and Vibration*, Vol. 193, No. 2, 1996, pp. 453–464. doi:10.1006/jsvi.1996.0295

[2] McEwan, M. I., Wright, J. R., Cooper, J. E., and Leung, A. Y. T., "A Combined Modal/Finite Element Analysis Technique for the Dynamic Response of a Nonlinear Beam to Harmonic Excitation," *Journal of Sound and Vibration*, Vol. 243, No. 4, 2001, pp. 601–624. doi:10.1006/jsvi.2000.3434

[3] McEwan, M. I., "A Combined Modal/Finite Element Technique for the Non-Linear Dynamic Simulation of Aerospace Structures," Ph.D. Dissertation, School of Engineering, Univ. of Manchester, Manchester, England, 2001.

[4] Muravyov, A. A., and Rizzi, S. A., "Determination of Nonlinear Stiffness with Application to Random Vibration of Geometrically Nonlinear Structures," *Computers and Structures*, Vol. 81, No. 15, 2003, pp. 1513–1523. doi:10.1016/S0045-7949(03)00145-7

[5] Hollkamp, J. J., Gordon, R. W., and Spottswood, S. M., "Nonlinear Modal Models for Sonic Fatigue Response Prediction: A Comparison of Methods," *Journal of Sound and Vibration*, Vol. 284, Nos. 3–5, 2005, pp. 1145–1163. doi:10.1016/j.jsv.2004.08.036

[6] Spottswood, S. M., and Allemang, R. J., "On the Investigation of Some Parameter Identification and Experimental Modal Filtering Issues for Nonlinear Reduced Order Models," *Experimental Mechanics*, Vol. 47, No. 4, 2007, pp. 511–521. doi:10.1007/s11340-007-9047-7

[7] Hollkamp, J. J., Gordon, R. W., and Spottswood, S. M., "Nonlinear Sonic Fatigue Response Prediction from Finite Element Modal Models: A Comparison with Experiments," Proceedings of the 44th AIAA/ASME/ASCE/AHS/ASC Structures, Structural Dynamics, and Materials Conference, AIAA Paper 2003-1709, 2003.

[8] Beberniss, T. J., Gordon, R. W., and Hollkamp, J. J., "The Effect of Air on the Nonlinear Response of a Plate," Proceedings of the 48th AIAA/ASME/ASCE/AHS/ASC Structures, Structural Dynamics, and Materials Conference, AIAA Paper 2007-2085, 2007.

[9] ABAQUS, Software Package, Ver. 6.7-EF1, Dassault Systems Simulia Corp., Providence, RI, 2007.

[10] Tiso, P., and Jansen, E., "A Finite Element Based Reduction Method for Nonlinear Dynamics of Structures," Proceedings of the 46th AIAA/ASME/ASCE/AHS/ASC Structures, Structural Dynamics, and Materials Conference, AIAA Paper 2005-1867, 2005.

[11] Tiso, P., Jansen, E., and Abdalla, M., "A Reduction Method for Finite Element Nonlinear Dynamic Analysis of Shells," Proceedings of the 47th AIAA/ASME/ASCE/AHS/ASC Structures, Structural Dynamics, and Materials Conference, AIAA Paper 2006-1746, 2006.

[12] Przekop, A., and Rizzi, S. A., "Nonlinear Reduced Order Random Response Analysis of Structures with Shallow Curvature," *AIAA Journal*, Vol. 44, No. 8, 2006, pp. 1767–1778. doi:10.2514/1.18868

[13] Gordon, R. W., and Hollkamp, J. J., "Reduced-Order Modeling of the Random Response of Curved Beams Using Implicit Condensation," Proceedings of the 47th AIAA/ASME/ASCE/AHS/ASC Structures, Structural Dynamics, and Materials Conference, AIAA Paper 2006-1926, 2006.

[14] Przekop, A., and Rizzi, S. A., "Dynamic Snap-Through of Thin Walled Structures by a Reduced Order Method," *AIAA Journal*, Vol. 45, No. 10, 2007, pp. 2510–2519.

doi:10.2514/1.26351
[15] Hollkamp, J. J., and Gordon, R. W., "Modeling Membrane Displacements in the Sonic Fatigue Response Prediction Problem," Proceedings of the 46th AIAA/ASME/ASCE/AHS/ASC Structures, Structural Dynamics, and Materials Conference, AIAA Paper 2005-2095, 2005.
[16] Wang, X. Q., Mignolet, M. P., Eason, T. G., and Spottswood, S. M., "Nonlinear Reduced Order Modeling of Curved Beams: A Comparison of Methods," Proceedings of the 50th AIAA/ASME/ASCE/AHS/ASC Structures, Structural Dynamics, and Materials Conference, AIAA Paper 2009-2433, 2009.
[17] Lee, J., "Topology of the Four-Mode Strain Energy of Thermally Buckling Plates," *Journal of Thermal Stresses*, Vol. 25, No. 9, 2002, pp. 813–857.
doi:10.1080/01495730290074441
[18] Yang, B., Mignolet, M. P., and Spottswood, S. M., "Modeling of Damage Accumulation for Duffing-Type Systems Under Severe Random Excitations," *Probabilistic Engineering Mechanics*, Vol. 19, Nos. 1–2, 2004, pp. 185–194.
doi:10.1016/j.probengmech.2003.11.015
[19] MATLAB, Software Package, Ver. 7.4, Mathworks, Inc., Natick, MA, 2007.

C. Cesnik
Associate Editor